Simulation of the dynamic response of high-speed line structures composed of granular or bituminous sub-ballast layers and comparison with in situ measurements from embedded instrumentation

Diana Khairallah, Olivier Chupin, Juliette Blanc, Pierre Hornych, Jean Michel Piau

Simulation of the dynamic response of high-speed line structures composed of granular or bituminous sub-ballast layers and comparison with in situ measurements from embedded instrumentation

Diana Khairallah[1], Olivier Chupin[1], Juliette Blanc[1], Pierre Hornych[1], Jean-Michel Piau[1]

（[1] Université Gustave Eiffel, Campus de Nantes, département MAST / LAMES, Allée des ponts et chaussées, 44344 BOUGUENAIS, France, juliette.blanc@univ-eiffel.fr）

Corresponding Author: Juliette BLANC, juliette.blanc@univ-eiffel.fr

Corresponding Author's Institution: Université Gustave Eiffel, Campus de Nantes, LAMES/MAST, Allée des ponts et chaussées, 44344 BOUGUENAIS, France

ABSTRACT

The “Brittany - Loire” high-speed line (HSL BPL), connecting the cities of Rennes and Le Mans is the first large-scale application, in France, of ballasted tracks with bituminous sublayer and varied subgrade conditions. To evaluate the behaviour of this new type of track structure, and validate the design assumptions, it was decided to set in place a monitoring system, to monitor the mechanical response of the track. For that purpose, three track sections were instrumented during construction using accelerometers, anchored deflection sensors, strain gauges and temperature probes.

The objective of this paper is to analyse the response of three instrumented track sections of the HSL BPL, either with a bituminous or a granular sublayer, and to model their response using a dynamic model, considering a viscoelastic multilayer structure subjected to moving loads, implemented in the ViscoRail software. From the numerical point of view, the objective was to verify the capacity of ViscoRail to simulate the response of the three BPL sections, using as much as possible a unique set of mechanical parameters, while considering the specificities of each sections. The comparison between the modelling results and the *in situ* measurements indicates that the model is able to reproduce the main features of the dynamic response of railway tracks. In particular, the role of the asphalt concrete layer, which tends to reduce vertical accelerations in the ballast layer is well reproduced by ViscoRail.

Keywords: Railway modelling, ballasted railways, asphalt concrete, monitoring

Author Accepted Manuscript published in Transportation Geotechnics, 35(2022)
https://doi.org/10.1016/j.trgeo.2022.100767

1. INTRODUCTION

In France, an important feedback on ballasted high-speed lines with granular sublayers allowed to improve track design rules and optimize maintenance operations (Lambert et al., 2011). More recently, the use of asphalt sublayers under the ballast has been identified as a possible solution for enhancing sustainability of track structures. Experience in different countries has shown that the behaviour of the overall structure is greatly improved by interposing a layer of asphalt concrete (GB for Grave Bitume, in French) between the ballast and the layer of unbound granular material (UGM). For instance, over the last decade, 322 km of sub-ballast layers have been built in new projects in the Midwestern United States, mainly for heavy freight traffic (Rose & Souleyrette, 2015). However, quantitative data about the mechanical response of railway tracks with asphalt sublayers is still lacking, especially for high speed lines, and analysis of the behaviour of these structures still needs investigation.

The "Brittany - Loire" high-speed line (HSL BPL) represents the first large-scale application in France of ballasted tracks with asphalt sublayers and varied subgrade conditions. This line includes 77 km of track with a granular sublayer (UGM) and 105 km of track with asphalt sublayer. The asphalt concrete layer aims in particular at increasing the stiffness of the track, improving its durability and reducing the amplitude of the vertical accelerations generated in the ballast layer by high-speed trains.

The implementation of a monitoring system on the BPL high-speed line seemed essential to improve knowledge of the behaviour of such railway tracks and evaluate the benefits of introducing an asphalt sublayer, as compared to classical construction techniques using UGM sublayers. The objective was also to validate the design assumptions for such structures, for future projects.

From the side of railway simulation, different track models have successively been developed to reproduce the dynamic behaviour of track structures under train loading. A distinction is usually made between analytical or semi-analytical models and numerical models. In general, analytical models are appropriate to predict the mechanical response at the level of the rails but not to study accurately the mechanics of the platform. Two main types of analytical models can be distinguished: models considering a continuous rail support on the foundation and models considering discrete supports formed by the sleepers.

Among the simplest 1D models, one can cite the models composed of Euler-Bernoulli beams modelling the rails, resting on a Winkler foundation (continuous distribution of elastic springs representing an equivalent soil). (Heckl, 2002; Nielsen & Igeland, 1995; Sheng et al., 2007; Yang et al., 2015) considered an evolution of this model: periodically spaced discontinuous supports to model the discrete supports provided by the sleepers. (Filippov, 1961) and (Krylov, 1995) replaced the Winkler foundation by an elastic half-space (3D). In this case, the Euler-Bernoulli beam rests continuously on this semi-infinite half-space. (Vostroukhov & Metrikine, 2003) replaced the semi-infinite solid medium by a viscoelastic layer of finite thickness resting on a non-deformable support. The Kelvin-Voigt model was used to describe this layer. The work of (Nielsen & Igeland, 1995) considered the irregularities of the track (sinusoidal defect at the rail surface, flattened wheel ...); the behaviour of the track was considered linear while that of the mobile vehicle was non-linear. (Liu et al., 2011; Xu et al., 2015) improved the representation of the foundation by using several springs in series to model each layer independently of the others.

To study the performance of the sublayers and the interactions between all the elements of the track, numerical models are often used (Semblat & Pecker, 2009). The discrete element method for example allows to model accurately the response of ballast, by taking into account its granular (discontinuous) nature, and the effective shape of the grains (Karrech, 2007; Saussine & Néel, 2014; Voivret et al., 2014; Zhou et al., 2013). However, this type of modelling is not suitable for evaluating the overall behaviour of the track, since the sublayer is generally represented as infinitely rigid (Voivret et al., 2016) (Voivret et al., 2016). Moreover, such models generally lead to high computation times.

Consequently, the numerical analysis of railway structures is frequently performed by means of the finite element method (FEM) which relies on continuum-based models. This type of approach makes it possible to describe the whole structure and to represent accurately the geometry of the rails and of the track, while analytical models use simplified representations (beams, springs...). For instance (Connolly et al., 2014; Hall, 2003; Kouroussis et al., 2011; Paixão et al., 2015) used Abaqus and Ansys softwares to model track response. Such models require large numbers of elements, significant pre-processing efforts and generally also lead to significant computation times and require large storage capacities. Still about continuum-based numerical approaches, one can find in the literature models involving the boundary element method (BEM) as for example those used in (O'Brien & Rizos, 2005), coupling FEM and BEM for the modelling of the subgrade (assumed of infinite thickness).

Back to the semi-analytical approaches, a model called ViscoRail was developed by (Chupin & Piau, 2011b, 2011a, Chupin et al., 2014). This 3D model is dedicated to the computation of the dynamic response of railways under moving loads and implements a multilayer structure. The behaviour of each layer can be considered elastic or viscoelastic, in the case of asphalt materials. This model provides a realistic description of the railway structure, keeping with the advantages of analytical/semi-analytical techniques. The assumption made in this model of considering the track ballast as a homogeneous elastic layer was deemed relevant as long as the reversible behaviour of the structure (i.e. under one load cycle) is addressed (Chupin et al., 2021).

In the present article, a full validation of the ViscoRail tool and the ability of this software to predict the dynamical (reversible) response of railways are addressed through quite exhaustive comparisons between simulations and in situ measurements carried out for different conditions.

The article mentioned above (Chupin et al. 2021) only shows an example of validation of the ViscoRail tool. The structure under consideration in this previous paper includes only elastic layers and the comparison between the simulations and measurements is carried out for the vertical accelerations only. It is stated in (Chupin et al. 2021) that the ViscoRail tool has been broadly and successfully compared to in situ measurements but without showing the results (apart from the few ones mentioned right above). In the present paper, the comparison between the simulations and measurements is presented into details and addressed for several types of structure whose one incorporates a viscoelastic bituminous layer.

The present paper also significantly extends the comparisons made in (Khairallah et al. 2020) by considering supplementary track sections and mechanical fields. In addition to deflections and accelerations, the comparison now includes the vertical strains in the unbound granular layers and the horizontal strains in the asphalt concrete layer. Moreover, three track sections of BPL, one with a granular sublayer, and two with asphalt sublayers, and with different subgrade conditions, are now analysed.

Because ViscoRail intended to be a design tool, the objective was also to evaluate whether the same input parameters, corresponding to a "reference" structure, can predict the mechanical response of all three sections, changing only the material properties of the layers which differ on each particular section. Hence proving the "intrinsic nature" of the ViscoRail modelling in terms of the reversible response of a railway structures.

Following the introduction, this paper is organised as follows: section 2 describes the high-speed line BPL, the instrumentation and the data processing of the collected measurements. Section 3 provides some basics of ViscoRail and details on the calibration of the model. Section 4 presents the results of the simulations of the three track sections with ViscoRail, and the comparison with the sensor measurements under a train pass. Finally, the main conclusions of the study are summarised in section 5.

2. THE HIGH-SPEED LINE "BRITTANY-LOIRE": INSTRUMENTATION AND DATA PROCESSING

The high-speed line Brittany - Loire (between Rennes and Le Mans, in the West of France) is the first large-scale application in France of the technique that consists in introducing an asphalt layer under the ballast. Here, this technique is used with varied subgrade conditions and was applied over 105 km of railway track (on the east part of the line) whereas 77 km with a granular sublayer (UGM) were built on the west part of the line. A high-performance asphalt concrete of class 4 (GB4), according to French standard NF EN 13-108-1, was used for this project. This material has a high elastic modulus (complex modulus at 15 °C and 10 Hz higher than 11000 MPa) and a high resistance to fatigue and rutting. The UGM, of type A according to French specifications, has a particle size of 0/31.5 mm. The track structure, with an asphalt sublayer, is built on a subgrade treated with lime and hydraulic binders. This treated natural soil is defined as the upper part of the earthworks (PST) in France. It is overlaid by a 15 cm thick UGM layer and a 12 cm thick asphalt layer. On the track structure with a granular sub-ballast layer, the UGM layer is 20 cm thick, and this structure includes an additional 35 cm thick subbase, consisting of soil treated with lime and hydraulic binder, over the PST, which is also treated (Figure 1).

Three instrumented sections are analysed in this paper: section 2, with a granular sublayer, and sections 1 and 4, with an asphalt concrete sublayer. The soil beneath the earthwork treated layer is composed mainly of shale on section 2 (with granular sublayer) and of yellowish clay with a broad sandy channel and scattered blocks on section 4 (with bituminous sublayer). Sections 2 and 4 are built on embankments. No water infiltration was detected on these two sections when a 6.5-m deep drilling campaign was conducted in September 2015. On the contrary, Section 1 with bituminous sublayer, is located in a cutting, and the subgrade, composed of yellowish fine sand, greyish, and greenish broad sandy channel showed water infiltration at 4.5 m depth, with a similar drilling made in September 2015."

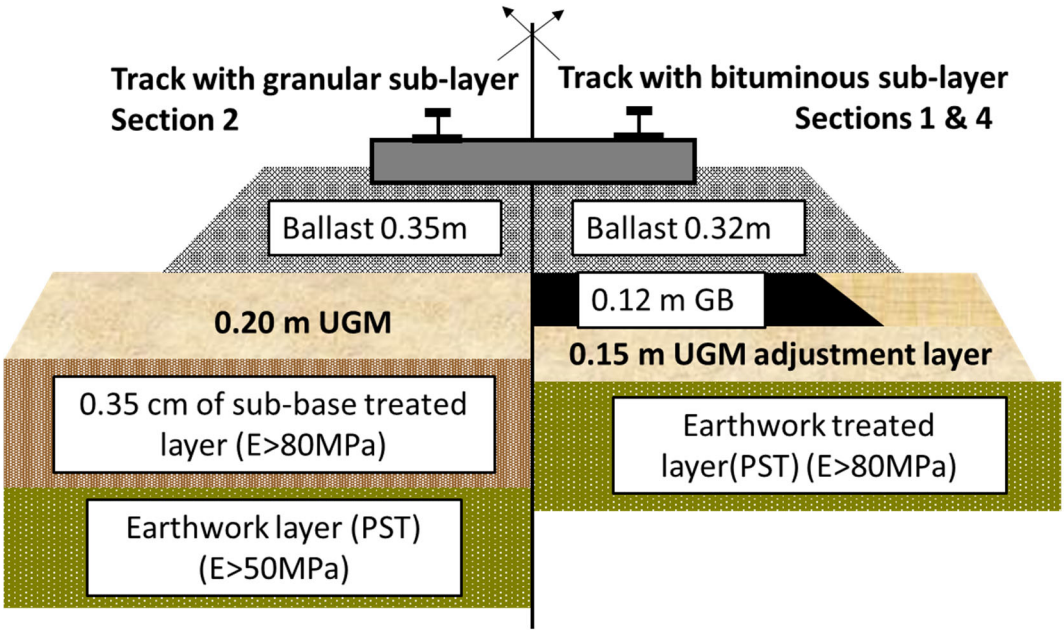

Figure 1. Structures of the BPL high-speed line with and without asphalt sublayer

2.1. Instrumentation of HSL BPL

To compare the responses of these different structures, the three sections were instrumented during the construction of the line. The aim of this instrumentation was to monitor and compare the mechanical response of these two types of structures used on the BPL HSL.

Section 2 (with a granular sublayer) is instrumented with 6 vertical strain gages (TML brand KM-100B) in the UGM layer, 16 accelerometers (reference 2210-005 of Alliantech brand) placed at different levels, 4 TDR moisture content probes (CS650-DS) in the UGM, 2 temperature sensors (KIMO PT100 probes) in the UGM layer, 2 anchored displacement sensors and a weather station.

Sections 1 and 4 (with an asphalt sublayer) are instrumented with 6 vertical strain gages in the UGM layer, 10 horizontal strain gages (TML brand KM-100HAS) in the asphalt layer, 8 accelerometers and 4 TDR moisture content probes in the UGM, 3 temperature sensors in the asphalt layer, 2 anchored displacement sensors and a weather station.

The full instrumentation set up on the various sites is detailed in (Khairallah et al., 2019a). Accelerometers are positioned at several depths in the structure: at the top of the asphalt concrete layer and at the top and bottom of the granular layer. The anchored deflectometers consist of a rod, anchored at a depth of 6 m, connected to an LVDT . The LVDT measures the relative displacement between the rod, supposed fixed, and a top cap, connected to the upper part of the sub-ballast layer (asphalt layer or granular layer, depending on the section). The deflectometers measure thus the total vertical displacement of the structure located under the ballast (UGM + subgrade for the section with granular sublayer or GB + UGM layer + subgrade for the section with asphalt sublayer). Moisture content probes monitor water content variations in the granular layer. Vertical strain gages monitor deformation levels of the UGM. Temperature probes are placed at the top and at bottom of the GB and UGM layers, to monitor temperature variations.

A plan showing the locations of the accelerometers, anchored deflectometers and strain gauges on section 2 (with granular sublayer), and sections 1 and 4 (with asphalt sublayer) is presented in Figure 2. The exact position of the sensors relatively to the sleepers is not known, because the instrumentation was installed during construction, before the sleepers were put in place. However, the longitudinal spacing between sensors of the same type (80 cm) was chosen slightly larger than the distance between sleepers (60 cm), thus leading to variable distances between the sensors and the sleepers.

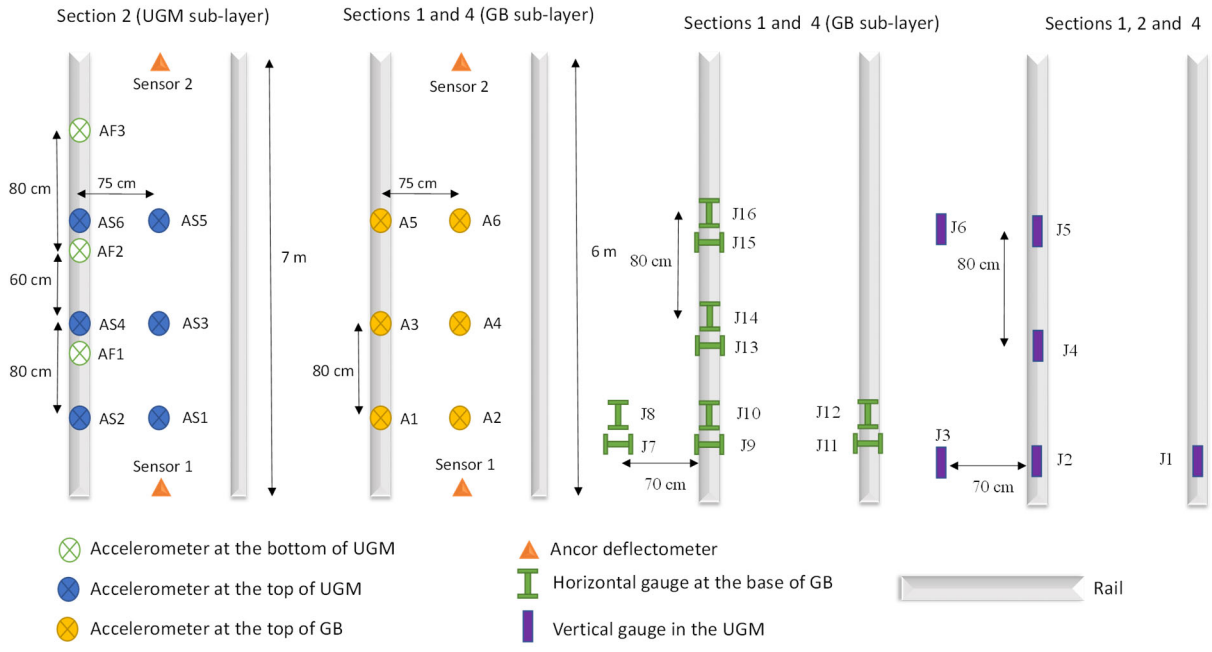

Figure 2. Instrumentation layout for accelerometers, displacement sensors, vertical strain gauges in UGM and horizontal strain gauges in GB layer, for the three instrumented sections

On each section, the sensors are connected to a data acquisition system enabling remote data transmission. Systems are autonomous in electricity and the power supply is provided by solar panels and batteries, for continuous operation without interruption. Data recorded on each section are transferred continuously via 4G network to a remote server. Results are stored in a relational database enabling fast-multi-criteria searches.

"Slow" measurements and "fast" measurements are performed on each section. Fast measurements concern accelerometers, vertical and horizontal strain gauges and anchored displacement sensors. They are triggered when the measured acceleration at the top of the first sublayer exceeds a certain threshold level, due to the passage of a train. This level is set to a very low value to ensure that all passages are recorded. The acquisition frequency is 2000 Hz (Le Cam et al., 2010; Le Cam et al., 2008). Slow measurements concern temperature probes, water content probes, data from the weather stations and anchored displacement sensors, recorded continuously every 5 minutes.

The data acquisition was divided in two phases. The ‘‘speed up test phase”, between November 2016 and January 2017, was the first acquisition phase before the opening of the track to commercial traffic. During this phase, the same train, with 10 cars and 13 bogies, circulated on the track at increasing speeds, ranging from 160 to 352 km/h. The second acquisition phase started in July 2017 with the opening of the line to commercial traffic, characterized by different high-speed trains circulating on the BPL track with an average speed of 320 km/h. This paper focusses only on the speed-up test phase.

Data from both acquisition phases was treated and evaluated. Measurements made on the granular and bituminous sections during the speed up phase are presented and compared in a previous paper (Khairallah et al., 2019a). The study clearly demonstrated that the presence of a bituminous sublayer reduces acceleration levels under the ballast, contributing to the stability of the ballast layer. The deflection levels are similar on sections 2 (with granular sublayer) and 4 (with bituminous sublayer). The deflection is lower on section 1 (with bituminous sublayer), due to the different soil (sandy soil).

Seasonal variations of layer temperatures, water contents and track settlements on the different instrumented sections, over a period of 30 months, were also studied in detail by (Khairallah, et al., 2019b). The role of the bituminous underlay to improve water drainage and protect the platform against rainwater infiltration has been clearly demonstrated. In addition, it was shown that the ballast layer plays an important role in protecting the sub-ballast layers against temperature variations.

In this paper, we focus on the modeling of the dynamic response of the instrumented sections of the BPL line under a single train passage (defined as the reversible response), using the ViscoRail software. After calibrating the model parameters, simulations carried out with ViscoRail are compared with different experimental results of the “speed up phase”.

2.2. Data processing

The BPL line was first put into service for a test phase, which lasted from November 2016 to January 2017. During these 3 months, a high-speed train travelled the line at speeds ranging from 160 km/h to 352 km/h. The train was composed of 8 cars and 2 locomotives (one at each end). The train being empty, it was possible to know the exact wheel loads . The loads of the carrying boogies vary between 14.5 tons and 15.5 tons.

For each train passage, the data acquisition system recorded the date and the time of the passage, the train velocity and the signals of the different sensors.

Filtering of the measurements according to a low-pass filter correlated to the train speed, V, was used to eliminate the dynamical effects observed at high frequencies. This allowed us to split the high-frequency effects related to the non-suspended masses, in particular wheel defects, from interacting effects of lower frequency between the train and the structure. The filtered measurements could then be compared to the signals computed by ViscoRail which assumes that the load intensity is constant (see further). The cut-off frequency, f_c, was calculated based on the "wheel wavelength" of approximately 3m and the train speed that define the "wheel frequency" denoting the frequency at which the same given point of a wheel (possibly the same given defect) comes into contact with the rail again after leaving it (f_c=V/2πR with R the wheel radius). The obtained frequency was increased by 10% to avoid significant signal loss. The same filter was applied to the deflection and vertical acceleration signals. However, it has been observed that this filtering barely affects the deflection signal measured by the anchored sensors confirming the "structural response nature" of the filtered signal. In contrast, the filtering reduces the magnitude of the vertical acceleration peaks taking them back to similar levels for bogies of the same weight. The split through this filter between low-frequency acceleration (of structural nature) and high-frequency acceleration (more variable and caused by the rolling stock) is then confirmed too. The acceleration peaks removed by filtering are of high magnitude but of short duration. Nonetheless, these could possibly affect grain rearrangements in the ballast layer, but such study is beyond the scope of the present paper and is not addressed herein.

After selection and filtering, a method called "superposition of carrier bogies" was used to process the measurements. For a given sensor and for a train passage at a known speed, the procedure consists in separating the signals corresponding to each carrier bogie, excluding the motor bogies and plotting all bogies signals starting from the same time origin. It is thus possible, for each sensor, to calculate the mean curve and the curves corresponding to +/- one standard deviation. Using this calculated mean curves, maximum and minimum accelerations and displacements, corresponding to a train passage, were calculated. This treatment is detailed in (Khairallah et al., 2019a). Mean curves and peak values of the sensor measurements were used for comparison with the ViscoRail simulations.

To illustrate this processing method, Figure 3 shows examples of filtered measurements made on section 4, with an asphalt sublayer, for a train speed of 320 km/h. The left figure shows an example of filtered vertical displacement (or deflection) measured using the anchored deflectometer. The deflection corresponds to the total vertical displacement of the layers under the ballast. The right figure shows a vertical acceleration signal.

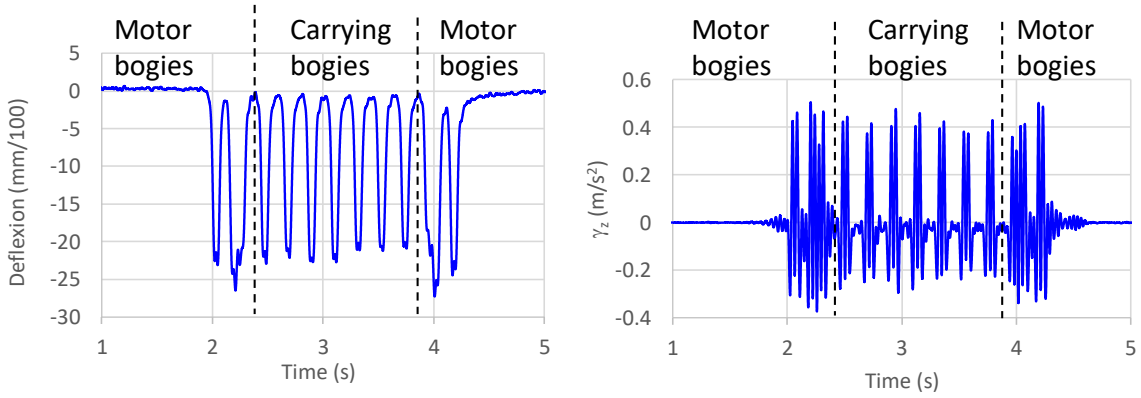

Figure 3. Filtered signals of vertical deflection (under the ballast) and vertical acceleration (for an accelerometer situated under the rail axis), example for a train passing on section 4 (with bituminous sublayer), on December 2nd, 2016, at 15h34, for a train speed of 320 km/h

Figure 4 presents the signals shown in Figure 3, treated with the method called "superposition of carrier bogies". Figure 4a shows the deflection signals, corresponding to the 7 carrier bogies, and the

calculated average signal. Figure 4b shows the 7 acceleration signals, and the calculated average signal. Positive values correspond to upward accelerations and negative values correspond to downward accelerations. The results show that the scatter of the filtered signals of the 7 bogies is low, which justifies using a mean signal for the comparisons with the modelling results.

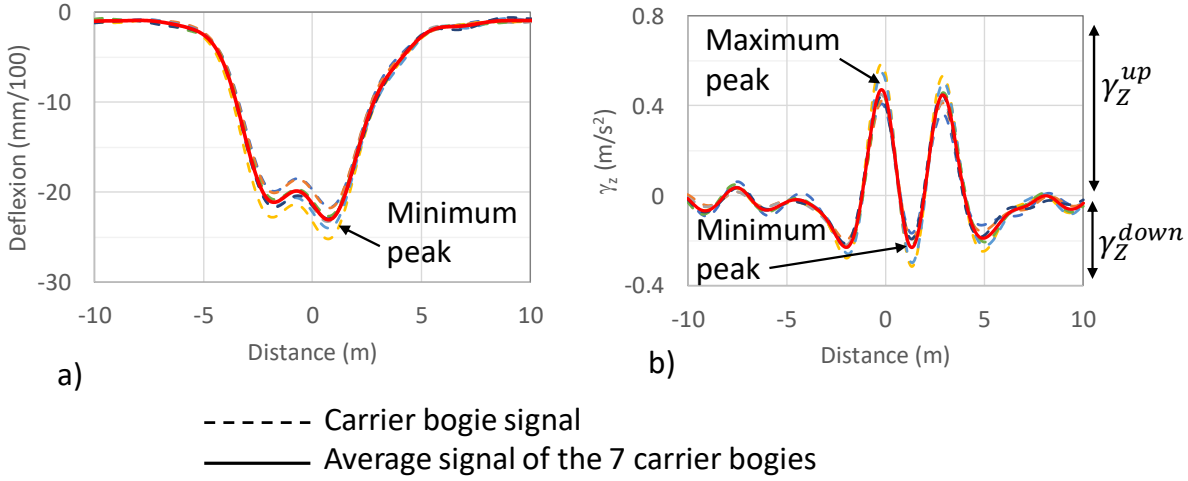

Figure 4. Vertical displacement (a) and vertical acceleration signals (b) (for an accelerometer situated under the rail axis) recorded under the seven carrier bogies, and calculated average signals, example for a train passing on section 4 (with bituminous sublayer), on December 2nd, 2016, at 15h34, for a train speed of 320 km/h

3. MODELING OF THE MECHANICAL RESPONSE OF THE THREE SECTIONS USING THE VISCORAIL SOFTWARE

3.1. Basics of ViscoRail

ViscoRail (Chupin & Piau, 2011b, 2011a) is a semi-analytical program dedicated to the computation of the dynamic (reversible) response of railway structures subjected to train loads represented as vertical forces applied on the rails, not varying with time but moving at constant speed. It does not handle the interaction between the vehicles and the railway track but it considers inertia effects induced by the specific mass of the structure layers. In ViscoRail, the track system is modelled as Euler-Bernoulli beams connected to the track sub-structure through elastic springs whose resulting force at the surface of the sub-structure is uniformly distributed over an area corresponding to the sleeper imprints. The distance between two consecutive springs is equal to the centre-to-centre distance between two sleepers. This connection that ensures load transfer to the sub-structure includes the sleepers and pads. The sub-structure is modelled by a semi-infinite multilayer medium whose layers can be either elastic or viscoelastic according to the Huet-Sayegh model in the case of bituminous materials. The Huet-Sayegh thermo-viscoelastic model (Huet, 1963; Huet, 1999; Sayegh, 1965) is well adapted to represent the behaviour of asphalt concrete materials. This rheological model is composed of two branches. One is made of two parabolic dashpots of exponent k and h (with $1 > h > k > 0$) in series with an elastic spring of stiffness E_∞. The second branch, in parallel to the other one, simply includes a spring of stiffness E_0. In the frequency domain utilized for the characterization of the reversible response of bituminous materials, the complex modulus E^* of this model is expressed by:

$$E^*\big(\omega\tau(\theta)\big) = E_0 + \frac{E_\infty - E_0}{1 + \delta(i\omega\tau(\theta))^{-k} + (i\omega\tau(\theta))^{-h}}$$

ω (rad/s) is the pulsation, δ is a non-dimensional parameter balancing the contribution of one dashpot with respect to the other in the global response and θ stands for temperature. τ is a time parameter used to account for the frequency-temperature superposition principle in the model:

$$a_T(\theta) = \exp(A_1\theta + A_2\theta^2), \tau(\theta) = \tau_0 a_T(\theta)$$

A_1, A_2 and τ_0 are constant parameters. An adapted viscoelastic model is necessary to compute accurately the stress and strain levels in the asphalt layer which behaviour depends on temperature and loading frequency in this layer (not easily inferred from the train speed). In ViscoRail, the problem is viewed as a coupled system composed of the tracks and the sub-structure, which is solved iteratively. The link between these two components is performed through the pressure distribution under the sleepers, $p(x,t)$. Concerning the sub-structure part and without going into the details, the solution at each iteration is obtained following the quasi-stationary approach which however is not straightforward since $p(x,t)$ varies in time depending on the location of the loads on the rails, due to the discontinuous distribution of the sleepers at surface of the sub-structure. As a consequence, a decomposition of this pressure distribution into loading waves moving at different speeds constant with time is considered. These are used as an input of the dynamics equations which are first solved in the wave number domain (for a semi-infinite layered domain which makes it easy to avoid wave reflection at the model boundaries) prior to applying an inverse fast Fourier transform to obtain the time response. This is performed using the software ViscoRoute© 2.0 (Chabot et al., 2010; Duhamel et al., 2005, Chupin et al., 2010). Then, the dynamic response to the full moving load is computed by recombination of the responses to each loading wave. For more information about the solution process implemented in ViscoRail, the reader is referred to (Chupin et al., 2014). The outputs of ViscoRail are the 3D mechanical fields in the structure (displacements, accelerations, strains…). These are usually represented as spatial profiles (for a given time) or time profiles (at a given location in the structure).

As a remark, given the assumptions made in ViscoRail, this tool is not meant to address the response of the structure to harmonic loading, the wheel-track interaction or to be used for the simulation of structures with flaws, especially because of the assumed periodicity and homogeneity of the model in the load moving direction.

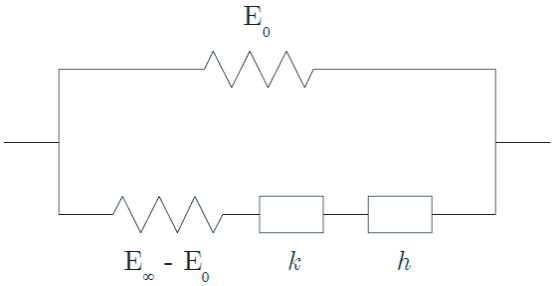

Figure 5. Huet-Sayegh rheological model

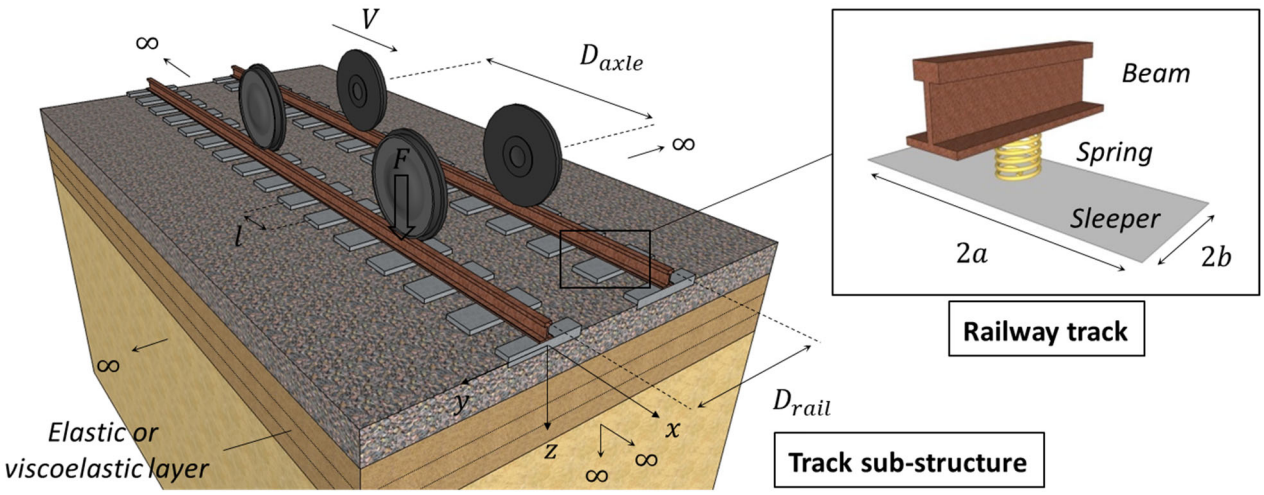

Figure 6. Railway track model illustrated by (Chupin & Piau, 2011b, 2011a).

3.2. Input data and determination of the unknown model parameters

Modeling HSL BPL structures using ViscoRail requires defining the model input parameters which are not all measured on site (e.g. granular layer and soil moduli...). To determine these unknown parameters, a back-calculation approach was used, which consisted in minimizing the difference between the measured and simulated response. For this purpose, measurements obtained on the granular section (deflections, strains and accelerations at different locations) for train velocities V = 160 and 320 km/h were selected.

Each layer i, of thickness e_i, is assumed composed of a homogeneous material of density ρ_i and of modulus E_i for the elastic layers. The Young modulus Er of the rails and their geometrical moment of inertia Ir around the y-axis are respectively fixed at 210,000 MPa and 3 × 10-5 m^4, values corresponding to the type of rails used on HSL BPL (UIC 60). On the BPL line, the rails are supported by mono-block sleepers whose footprint is approximated in ViscoRail by rectangles centered on the rails, and of surface $S = 2a \times 2b = 1.2 \times 0.3$ m^2 (Figure 6). Furthermore, the track gauge is taken equal to $Drail$ = 1.435 m and the center-to-center distance between two consecutive sleepers is l = 0.6 m. In the model, the load applied to the rails is a bogie with two axles, corresponding to a carrier bogie of the test train circulating during the speed up test phase. The bogie is assumed to move at a constant velocity V, in each calculation. Axles are spaced D axle = 3 m apart and the vertical load on each wheel is F = 80 kN (constant in time) ; the carrier bogie total load is equal to 320 kN. All of these parameters are used as inputs for ViscoRail.

The other model parameters to be determined for the simulations of the three BPL track sections (see Tables 2 and 3) are the Young moduli and Poisson ratios of the different layers considered as elastic in the model and the stiffness of the rail pads k_p. The asphalt material is considered viscoelastic, and is described by the Huet-Sayegh model. The model parameters used in the simulations (table 1) are calibrated from laboratory complex modulus tests performed on the GB4 material of the project, using the Viscoanalyse® software (Chailleux et al., 2006).

For the calculations, it is assumed that the Elastic moduli of the granular materials (UGM and ballast) are the same for the three HSL BPL sections studied in this paper. In addition, the Elastic modulus of the soil is assumed to be the same on sections 2 (with granular sublayer) and 4 (with bituminous sublayer) which rest on shale and clay soils respectively. A different soil modulus is used for section 1 (with bituminous sublayer), which lies on a sandy soil. To summarize, the three sections

are simulated considering the same set of parameter values. Only the Young modulus of the soil is adapted depending on the actual nature of the soil. A bituminous layer of known viscoelastic properties is also added, on sections 1 and 4.

TABLE 1. Huet-Sayegh model parameters for the bituminous layer

E_∞ (MPa)	E_0 (MPa)	k	h	δ	τ_0 (s)	A_1 ($°C^{-1}$)	A_2 ($°C^{-2}$)
32655	11	0.193	0.592	2.244	18.973	-0.397	0.00195

Finally, it is assumed that soil is 6 m thick and lies on a rigid bedrock. Beyond 6 m depth, the displacement of the structure is considered as negligible as recommended by the French pavement reinforcement guide (CEREMA-IDRRIM, 2016). The Poisson ratio is taken equal to 0.4 for all the layers. This value is chosen to help avoiding tensile stresses in the unbound granular layers which are modelled according to a linear elastic constitutive law.

To determine the unknown parameter values, the following realistic ranges of variation were considered for each parameter:

- Ballast layer modulus $E_{ballast}$: between 150 and 600 MPa
- Granular sublayer modulus E_{UGM} : between 200 and 1000 MPa
- Cement-treated capping layer modulus E_{CF} : between 400 and 5000 MPa
- Soil modulus E_{soil} : between 80 and 200 MPa
- Stiffness of the rail pads k_p : between 50 and 150 MN/m.

These ranges were discretized into several values and simulations, for V=160 and 320 km/h, were run for the cross values hence obtained for the different parameters. This resulted in many simulations among which that leading to the smallest difference between the simulations and the filtered measurements according to a given criterion was selected as defining the parameter values. This criterion was based on the maximum in absolute value of the deflection, the vertical acceleration at the location of the accelerometers and the vertical strain in the UGM layer at the location of the strain gauges. As shown further, this choice led at large to a satisfying comparison between the simulations and the measurements. In particular, the calibrated model was able to properly predict the response of the different structures for all the considered speeds (*e.g.* in terms of vertical acceleration). The computed quantities exhibiting the most difference with the measurements were generally not included in the aforementioned criterion indicating that its choice could be somehow adapted for a better accuracy of the simulations. Nonetheless, a better way to achieve more accurate results would be to calibrate the unknown parameters from testing.

The result of this calibration is shown in Tables 2 and 3 that summarize the characteristics of the three track sections used in the simulations detailed in the next section.

TABLE 2. Geometrical and mechanical characteristics of the model used for the structure with granular sublayer (section 2)

	ρ ($kg.m^{-3}$)	E (MPa)	ν	e (m)
Ballast	1800	250	0.4	0.30
UGM layer	1800	860	0.4	0.20
Cement treated capping layer	1800	2750	0.4	0.35
Soil	1800	160	0.4	6.0
Bedrock	1800	rigid	0.4	∞
Stiffness of the rail pads: $k_p = 100\ MN/m$				

TABLE 3. Geometrical and mechanical characteristics of the model used for the structure with asphalt sublayer (sections 1 and 4)

	ρ (kg.m^{-3})	ν	e (m)	Section 4 (clay soil) E (MPa)	Section 1 (sandy soil) E (MPa)
Ballast	1800	0.4	0.3	250	250
GB sublayer	1800	0.4	0.12	Huet-Sayegh model (lab values)	Huet-Sayegh model (lab values)
UGM layer	1800	0.4	0.15	860	860
Cement treated capping layer	1800	0.4	0.35	2750	2750
Soil	1800	0.4	6.0	160	80
Bedrock	1800	0.4	∞	rigid	rigid
Stiffness of the rail pads: $k_p = 100\ MN/m$					

Some comments can be made about the back-calculated layer moduli:

- The stiffness of the capping layer is high (2750 MPa). This value is consistent with the laboratory study performed by Preteseille et al.(2014) and Preteseille & Lenoir (2015) on different types of soils from the BPL line, treated with lime and cement, which led to modulus values up to 6000 MPa.
- The UGM modulus can be considered as dependent on the stiffness of the lower layers on which it is built. The high modulus value of 860 MPa of the UGM can therefore be explained by the presence of the treated capping layer.
- According to Chupin et al. (2021), the modulus of the ballast layer depends on the layer on which it is laid on. The value of 250 MPa obtained here is consistent with the range of values between 120 and 630 MPa considered by Fortunato (2005).

4. COMPARISON OF VISCORAIL CALCULATION RESULTS WITH SENSOR MEASUREMENTS

The ViscoRail computations were performed for the three sections with an asphalt sublayer and a granular sublayer and compared with the sensor measurements recorded during the speed up test phase.

The speed up phase lasted between November 2016 and January 2017. Temperature variations during this period were limited. The average temperature in the asphalt concrete layer was 7 °C (with a minimum temperature of 2°C and a maximum temperature of 10°C). Consequently, all the signals recorded during this period can be compared , neglecting the influence of temperature variations on the stiffness of the asphalt layer. Therefore, the ViscoRail simulations were performed considering a constant temperature of 7°C in the asphalt layers.

The computations were carried out for four different traffic speeds: V = 160, 240, 320 and 350 km/h on section 2 and section 4. For section 1, the computations were performed for a speed of 160 km/h only, because experimental measurements were available only for 160 km/h on this section, located at an extremity of the lane.

The loading considered in the simulations is a typical high-speed train carrier bogie composed of two axles spaced 3m apart and loaded at 160 kN each (80 kN per wheel). In the calculations, two different positions of the wheels were considered: A first position xF1 where the wheels are right above sleeper centers; for this position, the coordinates of the wheels are $\{0, 3m\}$. A second position xF3 where

the wheels are located at midpoint between two sleepers. For this position, the coordinates of the wheels are $\{0.3\ m, 3.3m\}$ (see figure 7).

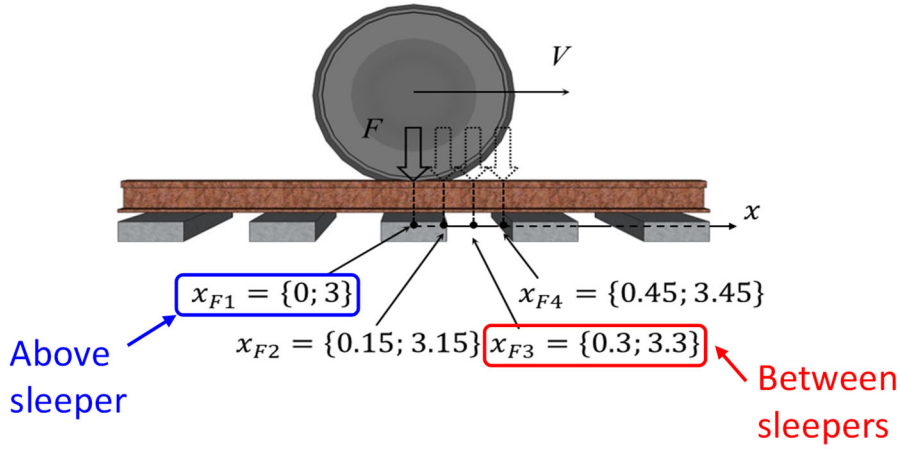

Figure 7. Load positions (x_F) (adapted from Martin, 2014)

4.1. Comparison of measured and calculated deflections

The deflection signals obtained from ViscoRail are compared with those from the anchored deflectometer located at the top of the GB layer in the asphalt section and at the top of the UGM layer in the granular section.

Figure 8 compares the average signals of the deflectometers, located between the rails, with the modeling results for section 2 (with granular sublayer) and section 4 (with bituminous sublayer) at V=320 km/h. Figure 8b shows that ViscoRail predicts correctly the deflection signal both in shape and in amplitude for the bituminous section. Concerning the granular section, the amplitude of deflection is well reproduced by ViscoRail but the shape of the computed signal differs slightly from the measured signal, in particular between the two peaks oriented downwards (Figure 8a). However, it should be noted that the objective of the authors was to use as much as possible the same model parameters for all the sections, as it would be done for design.

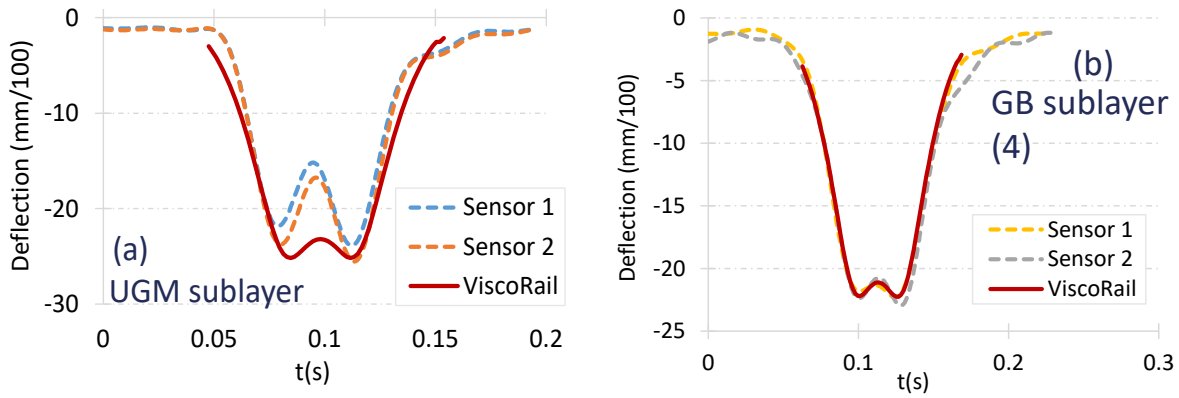

Figure 8. Comparison between predicted and measured deflection signals for (a) section 2 (with granular sublayer) and (b) section 4 (with bituminous sublayer) at V = 320 km/h.

Table 4 presents the comparison between the maximum values of deflection computed with ViscoRail and those measured on the asphalt sections and the granular section, for two different train speeds (V=160 km/h and V=320 km/h). The measurements indicate no variation of the deflection level with speed for section 2 (with granular sublayer) and section 4 (with bituminous sublayer). The calculated maximum deflection values for these two speeds are very close to the measurements. The numerical results exhibit a very slight increase of deflection with speed due to inertia forces. This increase is obtained for both structures even though asphalt layers get stiffer as speed increases (for the GB sections). Overall, the measured deflections are very low (between about 23 mm/100 and 25 mm/100) indicating a very good performance of the track.

For section 1 (with bituminous sublayer), the calculated maximum deflection value is very close to the measurement too (for V=160 km/h). As observed on the measurements, the deflection value calculated on this section is higher than the values calculated on sections 2 and 4, due to the lower modulus of the soil (80 MPa).

TABLE 4 Comparison of measured and predicted maximum values of deflection, for two train velocities

		V= 160 km/h		V= 320 km/h	
		Measured deflection (mm/100)	Deflection Predicted with ViscoRail (mm/100)	Measured deflection (mm/100)	Deflection Predicted with ViscoRail (mm/100)
Clay soil	UGM section 2	24.3	24.9	25.1	26.4
	GB section 4	23.4	22.1	23.3	23.2
Sandy soil	GB section 1	38.0	40.0	-	-

To extend the comparison, Figure 9 shows the maximum deflection values obtained with ViscoRail for the four passage speeds 160, 240, 320 and 350 km/h and for the two wheels positions, under sleepers and between the two sleepers, on granular section 2. The experimental data show that there is no change in deflection with speed, which is quite well rendered by the simulations. The observations are exactly the same for section 4 with a bituminous sublayer.

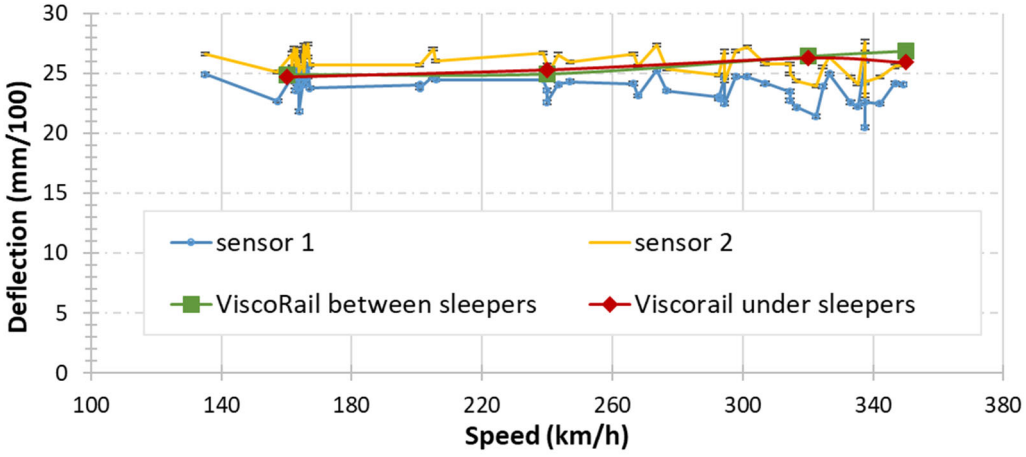

Figure 9. Comparison of the measured and calculated maximum deflections, for the two load positions x_{F1} and x_{F3} (granular section).

The ViscoRail model is thus able to reproduce well the measured deflections, for structures with different types of soil and with granular or bituminous sublayers, for different speeds.

4.2. Comparison of measured and calculated vertical accelerations

4.2.1. Section 4 with asphalt concrete sublayer

The vertical acceleration signals obtained from ViscoRail are compared with those from the accelerometers located at the top of the GB layer in section 4. The comparison is made for two train speeds: V = 320 and 160 km/h.

Figure 10 compares the average signals of accelerometers A1, A3 and A5 located under the axis of the rail (graphs (a) and (c)) and accelerometers A2, A4 and A6 located between the rails (graphs (b) and (d)) with the modeling results. The graphs show that ViscoRail predicts correctly the accelerometer signals both in shape and in amplitude for the two speeds.

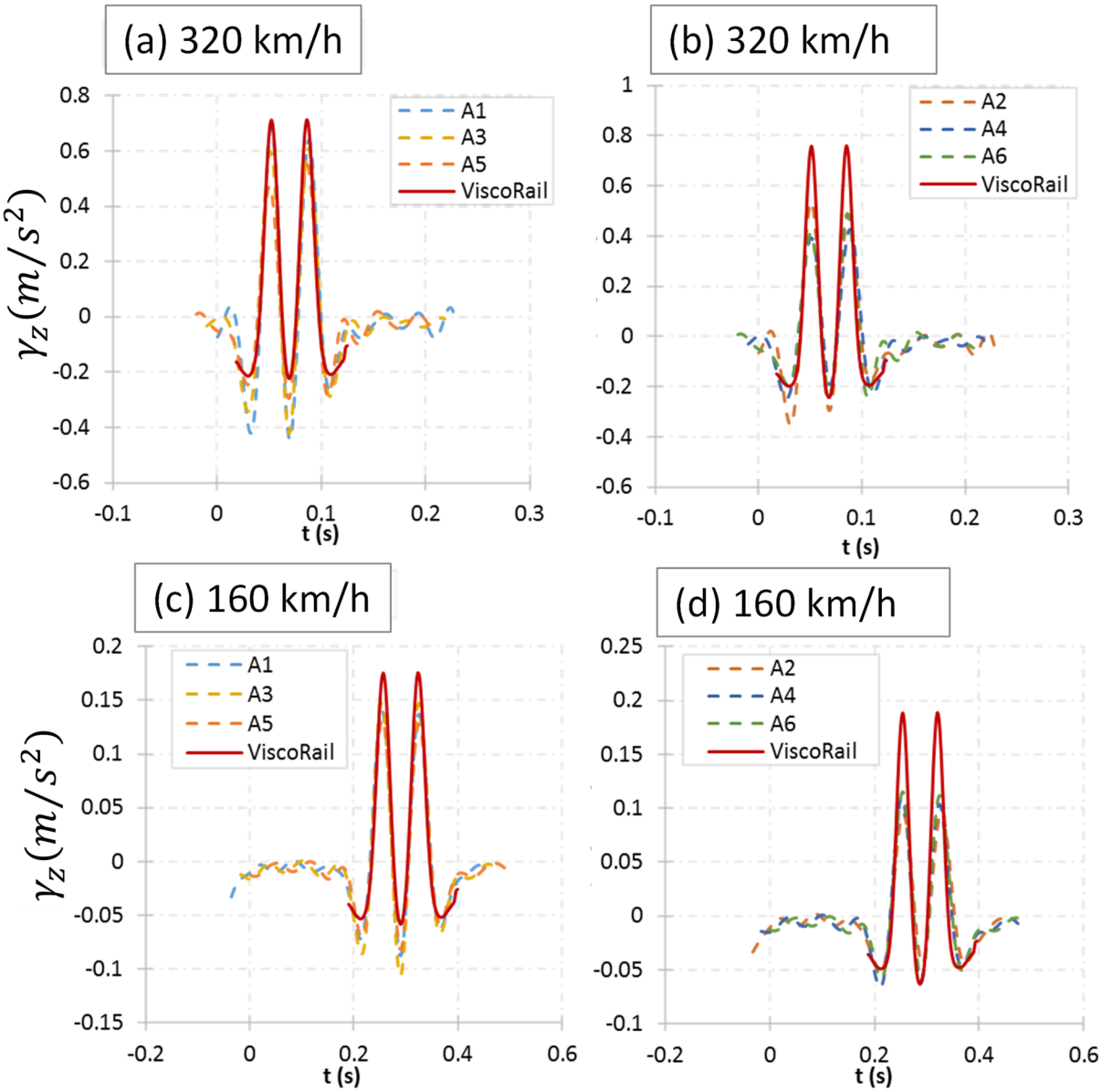

Figure 10. Comparison between measured and calculated vertical acceleration signals at the top of the GB layer (a) under the rail axis at V = 320 km/h, (b) between the rails at V = 320 km/h, (c) under the rail axis at V = 160 km/h and (d) between the rails at V = 160 km/h (adapted from Khairallah et al., 2020)

To illustrate the effect of the train speed on the vertical acceleration in the track structure, Figure 11 presents a comparison between the maximum measured and calculated values of the upward and downward accelerations at the top of the GB layer between the rails, for speeds varying between 160 and 352 km/h. Again, the calculations are carried out for two load positions xF1 = {0; 3} m (load applied on the sleepers) and xF3 = {0.3; 3.3} m (load between two sleepers) as shown in Figure 7. The results obtained for the two positions are very similar.

The ViscoRail software renders the non-linear increase of accelerations with speed. The positive (upward) accelerations are slightly overestimated; while the the negative (downward) accelerations are predicted correctly. Overall, the vertical accelerations under the ballast are quite small, with maximum levels around 1 m/s^2.

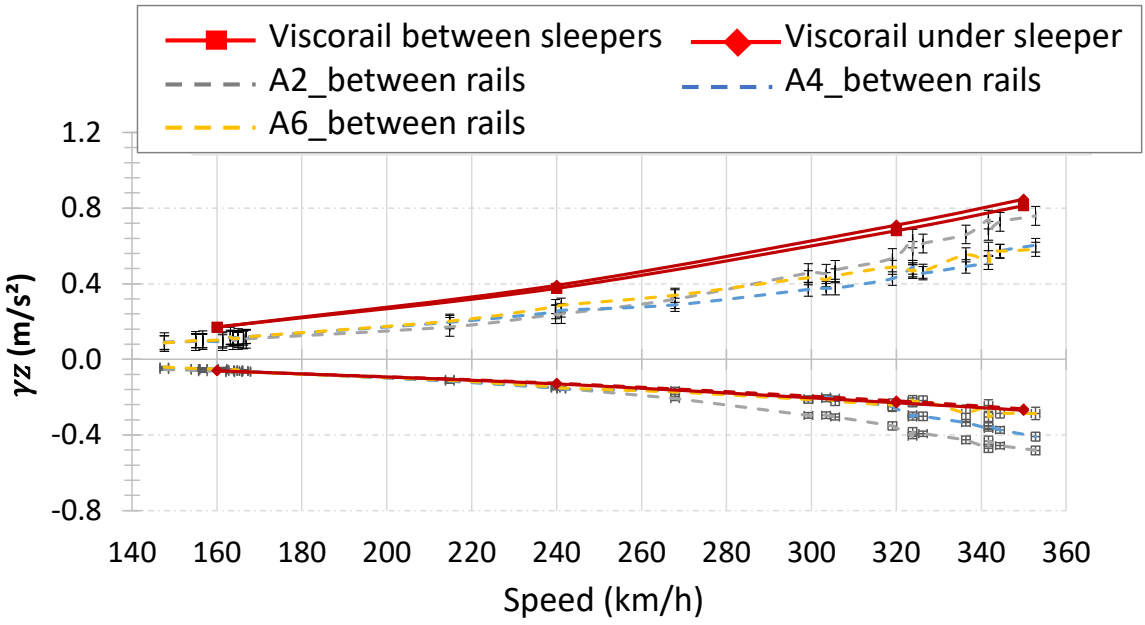

Figure 11. Comparison of calculated and measured maximum accelerations at the top of the GB layer between the rails, on the asphalt section, for two load positions, x_{F1} = {0; 3} (above sleeper) and x_{F3} = {0.3; 3.3} (between sleepers)

4.2.2. Section 1 with bituminous sublayer

Table 5 presents the comparison of measured and calculated maximum and minimum values of vertical acceleration, at the top of the bituminous layer, for section 1, at the speed of 160 km/h.

Again, the calculations are carried out for two load positions xF1 = {0; 3} m (load applied on the sleepers) and xF3 = {0.3; 3.3} m (load between two sleepers) as shown in Figure 7. The results obtained for the two positions are very similar.

The ViscoRail software predicts well the levels of the positive (upward) accelerations under the ballast layer, while the negative (downward) accelerations are somewhat underestimated. For the speed of 160 km/h, the measured and computed vertical accelerations under the ballast are quite small, with maximum levels around 0.24 m/s^2.

TABLE 5 Comparison of measured and calculated maximum and minimum values of vertical acceleration, at the top of the bituminous layer, for section 1, at the speed of 160 km/h

	Under the rail axis				
	Measured acceleration (m/s^2)			Calculated acceleration (m/s^2)	
	A2	A4	A6	Under sleeper	Between sleeper
γ_z^{up}	0.20	0.22	0.24	0.22	0.21
γ_z^{down}	0.11	0.13	0.15	0.06	0.06
	Between the rails				
	Measured acceleration (m/s^2)			Calculated acceleration (m/s^2)	
	A1	A3	A5	Under sleeper	Between sleeper
γ_z^{up}	0.19	0.22	0.22	0.21	0.20
γ_z^{down}	0.11	0.13	0.15	0.07	0.07

4.2.3. Section 2 with UGM sublayer

The average signals of HST passages on HSL BPL, for all the accelerometers installed at the top of the granular layer of section 2, are compared with the signals calculated under the ballast with ViscoRail in Figure 12. This figure shows a comparison between the average signals of accelerometers AS2, AS4 and AS6 located under the rail axis (graphs (b) - (d)), and accelerometers AS1, AS3 and AS5 situated between the rails (graphs (a) - (c)), and the signals calculated with ViscoRail for these same positions, for 2 HST circulations in January 2017, at V = 320 and 160 km.h^{-1} (at the temperature of about 7°C). The dashed lines correspond to the average curves of the measurements, while the red curve represents the calculation results. The software reproduces well the shape of the measured vertical acceleration signals, but slightly underestimates the maximum accelerations, in particular those directed downwards (negative).

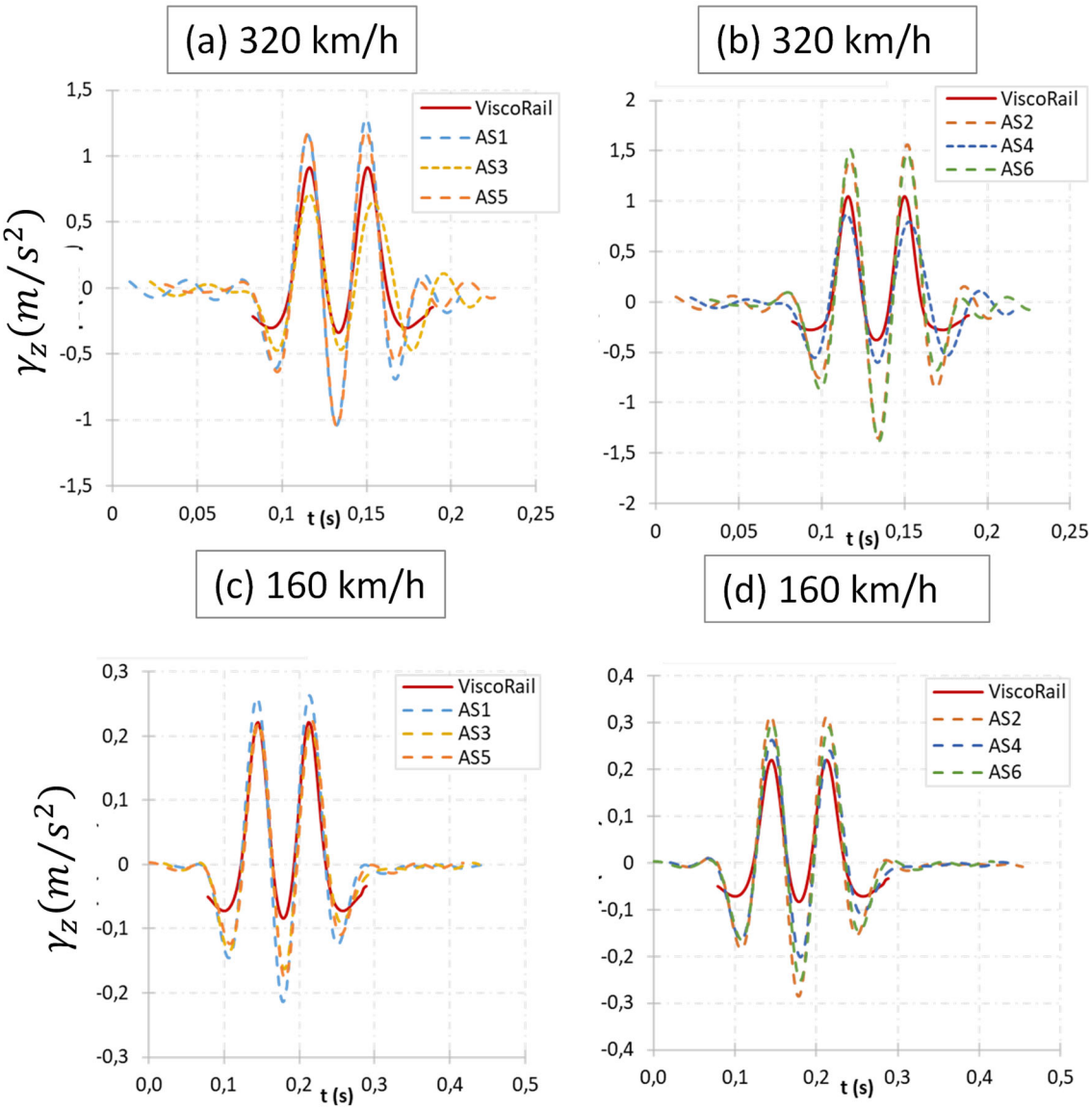

Figure 12. Comparison between predicted and measured longitudinal acceleration signals at the top of the UGM layer (a) between the rails at V = 320 km/h (b) under the rail axis at V = 320 km/h, (c) between the rails at V = 160 km/h and (d) under the rail axis at V = 160 km/h

As for section 4, the maximum accelerations calculated with ViscoRail are compared with the peak accelerations recorded by the sensors. The calculations are carried out for four train speeds: V = 160, 240, 320 et 350 km.h^{-1}. Figure 13 compares the measured and the calculated acceleration for all the velocities, (a) under the axis of a rail and at the top of the UGM layer ($\{x; y; z\} = \{0; 0; 0.3\}$) and (b) at mid-distance between the rails at the top of the granular layer ($\{x; y; z\} = \{0; 0.75; 0.3\}$). Both the positive peak accelerations (directed upwards) and the negative peak accelerations (directed downwards) are displayed.

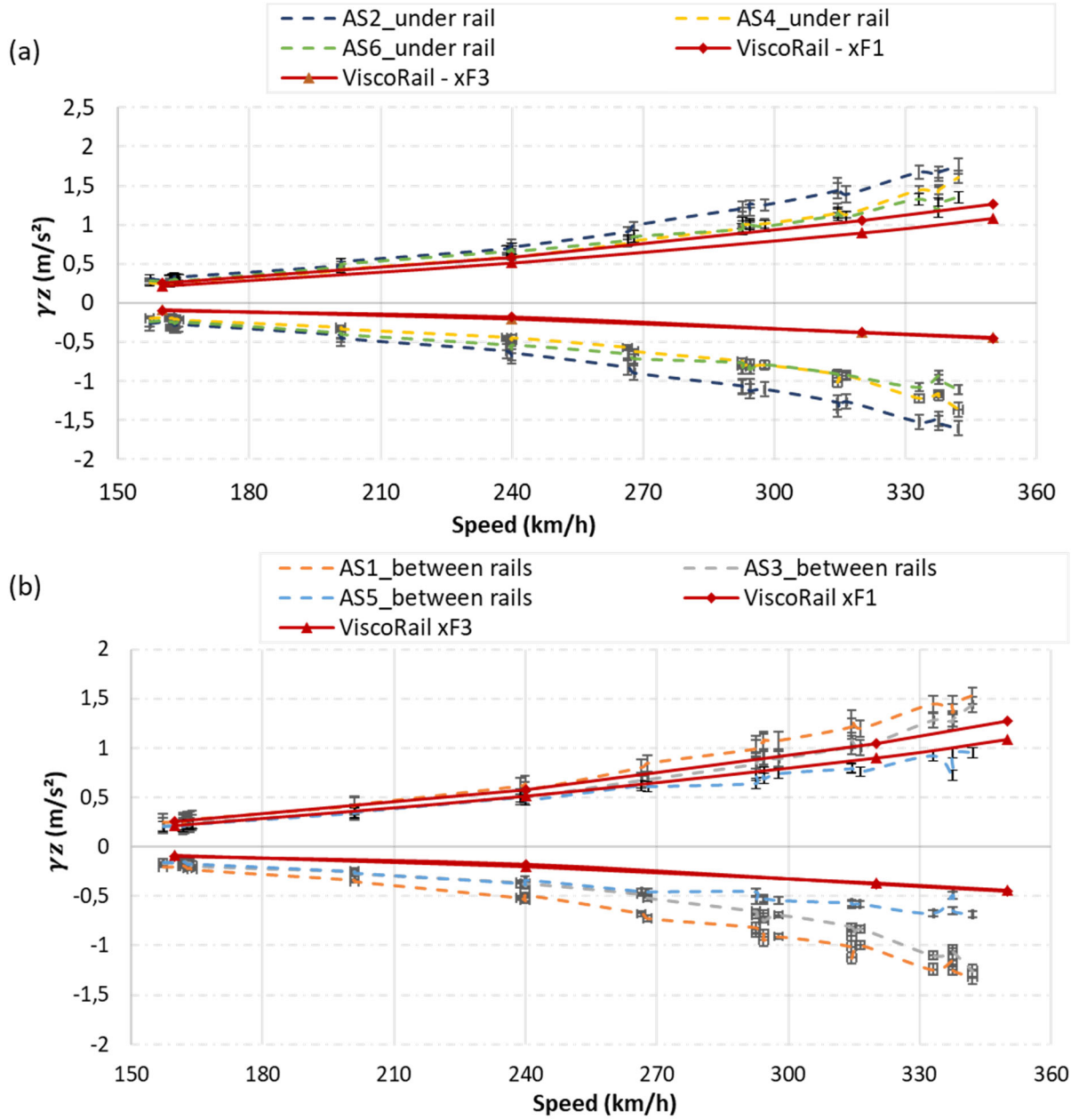

Figure 13. Comparison between peaks of measured and calculated vertical accelerations at the top of the UGM layer on section 2 with granular sublayer: (a) under the rail axis, (b) between the rails.

It can be noticed in Figure 13 that:

- the upwards and downwards acceleration curves calculated with ViscoRail for the two load positions $xF_1 = 0$ and $xF_3 = 0.3$ m are very similar.
- The same trend in terms of increase of the vertical acceleration with train speed is observed on the experimental data and the ViscoRail computations.
- As already mentioned, ViscoRail reproduces the positive (upward) accelerations very well, but underestimates the negative (downward) accelerations.
- The maximum acceleration levels (around 1.5 m/s^2) obtained for this section with a granular sublayer are significantly higher than those measured on the section with a bituminous sublayer. Nevertheless, the accelerations remain at a relatively low level that can be considered as safe with respect to the risk of ballast settlement under the repeated passage of HST.

On section 2, the vertical accelerations were also measured at the bottom of the granular sublayer. The accelerometers were placed under the rail axis, at 0.45 m in depth. Figure 14 compares the accelerations calculated with ViscoRail, for $\{x; y; z\} = \{0; 0; 0.45\}$ and for the two load positions xF_1 and xF_3, with data measurements of the three accelerometers AF1, AF2 and AF3 (dashed lines). The experimental results show that vertical accelerations increase non-linearly with train speed, and are higher at the top of the granular layer than at the bottom. The same observation can be made for the numerical results. Attenuation of the vertical acceleration with depth seems well captured by ViscoRail.

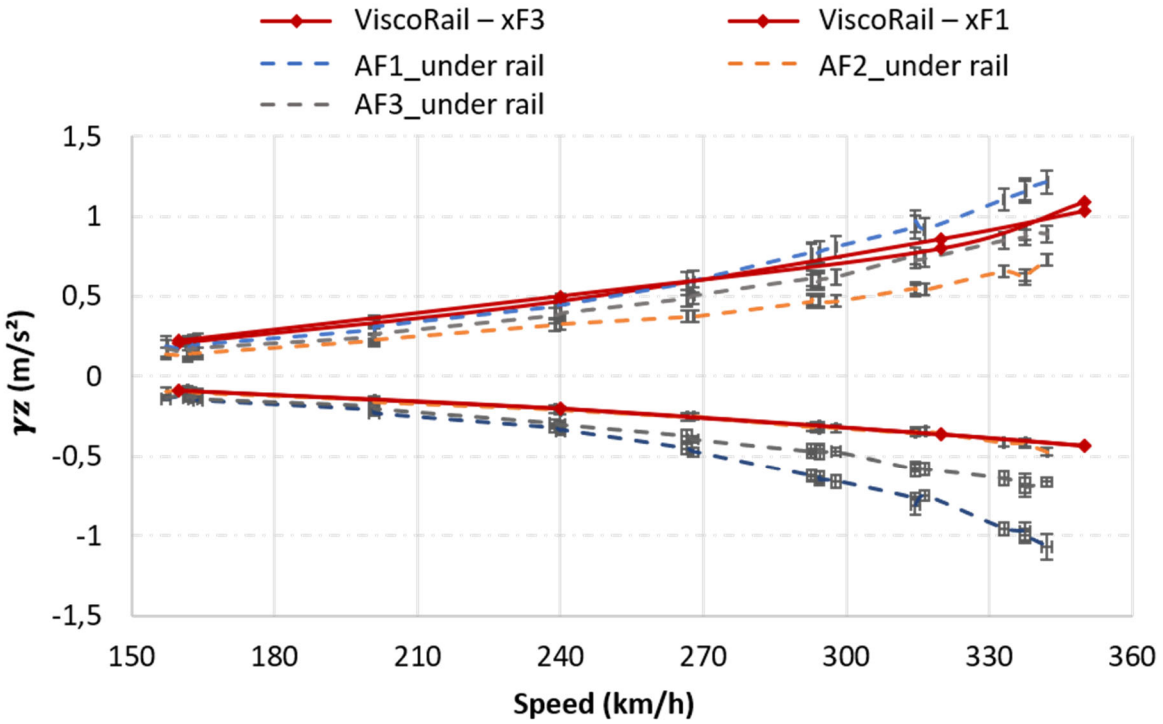

Figure 14. Comparison between peaks of measured and calculated vertical accelerations, under a rail axis, at the base of the UGM layer, in section 2, for two load positions x_{F1} = {0; 3} and x_{F3} = {0.3; 3.3}.

4.3. Modeling of vertical and horizontal strains

4.3.1. Vertical strains in the UGM layer

The vertical strains measured at the bottom of the UGM layer using strain gauges (J1 to J6) are compared with calculated values in Figure 15 (for section 2) and in Figure 16 (for section 4), for the four considered speeds. The strains are calculated for two positions: under a sleeper and between two sleepers. The results in Figures 13 and 14 show that the calculated vertical strains are of the same order of magnitude as the measured ones, slightly higher though, but not significantly given the low vertical strain levels (less than 20 µstrain) reached in the granular layer, compared with the accuracy of these gauges which is about 10 µstrains. In comparison, in road pavements, vertical strains in granular subbase layers are generally of the order of several hundred microstrains. The measured and predicted vertical strains are not affected by the train speed.

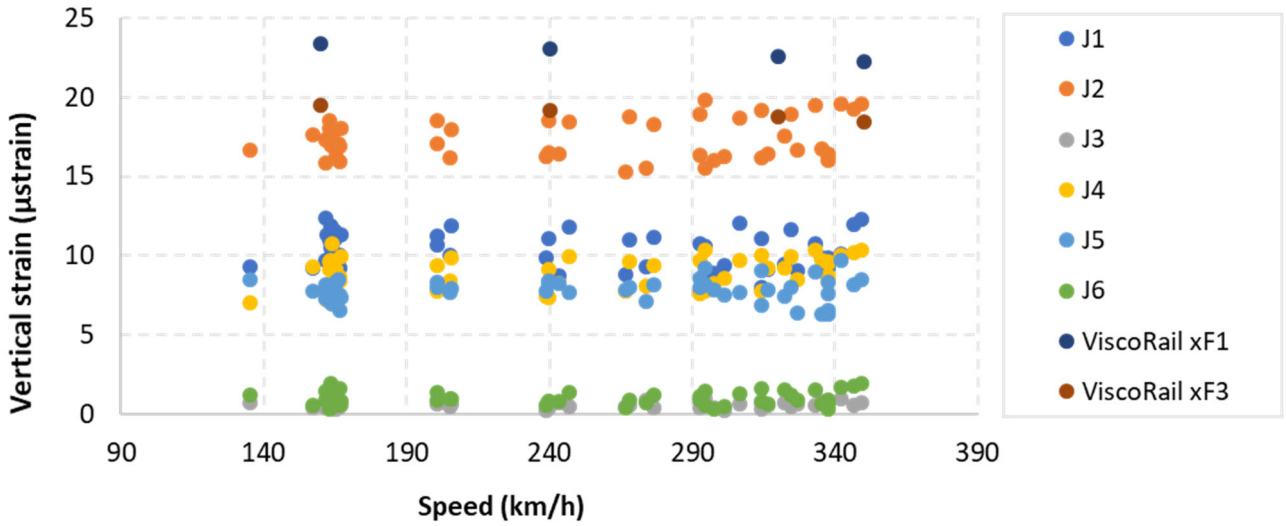

Figure 15. Comparison between peak values of vertical strains measured with the vertical gauges installed in the UGM layer in section 2 (with granular sublayer) and values calculated with ViscoRail for two load positions, x_{F1} = {0; 3} and x_{F3} = {0.3; 3.3}

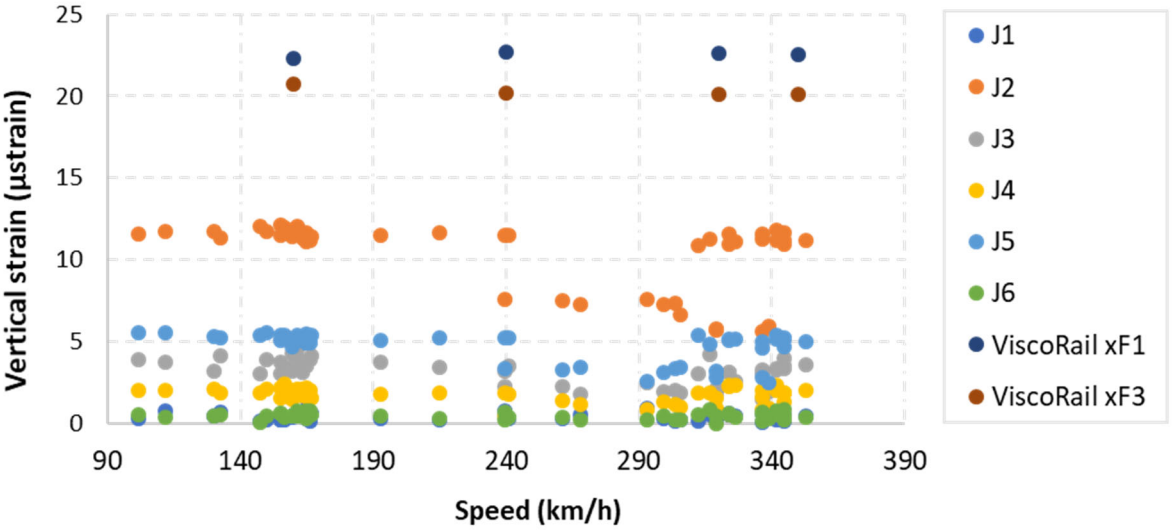

Figure 16. Comparison between peak values of vertical strains measured with the vertical gauges installed in the UGM layer in section 4 (with bituminous sublayer) and values calculated with ViscoRail for two load positions, x_{F1} = {0; 3} and x_{F3} = {0.3; 3.3}

4.3.2. Horizontal strains in the bituminous layer

Similarly, the measured and calculated transversal and longitudinal strains at the bottom of the bituminous layer are also extremely low. Indeed, with ViscoRail, the calculated transversal strains are less than 2 µstrain and the calculated longitudinal strains are less than 6 µstrain, for all train speeds. These values are consistent with the experimental measurements of the horizontal gauges installed at the bottom of the GB layer, for both sections, which reported maximum values of 14 µstrain and 11 µstrain in the transverse and the longitudinal directions, respectively. The difference is not significant, due to the very small magnitude of the measured strains, to the uncertainty regarding the longitudinal position of the sensors relative to the sleepers, and to the accuracy of the gauges (around 10 µstrain).

Because the sensors were installed before putting in place the sleepers, it was not possible to control the position of the sensors relative to the sleepers. However, the results can be considered very satisfactory, since ViscoRail confirms the very small strain values measured in situ.

In view of the very low strain levels recorded at the bottom of the GB layer, one can conclude that there is no risk of fatigue of the bituminous layer. For asphalt materials, two-point bending fatigue tests performed on these materials (according to standard NF-EN-12697-26) lead to determine a fatigue parameter $\varepsilon_{6,}$ which represents the tensile strain leading to fatigue failure for 1 million load cycles, for a standard test performed at 10 °C and 25 Hz. For the GB4 material used on the track, the value of the tensile strain parameter ε_6, is of the order of 100 μstrain (at 10°C). Therefore, on the track, with strain levels under 15 μstrain, the risk of fatigue of the bituminous layer appears negligible.

5. CONCLUSION

Three sections of the BPL high-speed line, with granular sublayer and asphalt sublayer and different types of soil have been largely instrumented in order to study their mechanical response under high-speed train loading.

The behavior of the three sections was modeled using the ViscoRail software developed to simulate the dynamic response of railway structures. A calibration procedure was used to determine the model parameters that could not be inferred from testing. Deliberately, the same set of model parameters was used for the three sections (expect when the layers were different), to assess the predictive ability of Viscorail to simulate the dynamical response of railway structures. Indeed, similar assumptions would be made for design applications.

With this approach, reasonably good predictions of the response of the three structures were subsequently obtained, for different speeds and different mechanical fields examined at several locations in these structures, except for the negative accelerations on section 2, which were underestimated. The difference in maximum accelerations between the granular and the bituminous sections was also confirmed by the calculations. Measurements recorded for speed levels varying between 160 and 352 km/h have shown that the introduction of a bituminous sublayer under the ballast reduces significantly (approximately by a ratio of two) the vertical accelerations under the ballast

All these results are very encouraging and confirm that the ViscoRail semi-analytical model, based on a simplified representation of the railway track (rails are represented by beams connected by springs to a semi-infinite multilayer structure), can predict correctly the dynamic response (reversible) of ballasted track structures, with and without bituminous sublayers, under a load of constant magnitude moving at constant speed. ViscoRail therefore appears as an efficient simplified tool for fast calculations of the response of railway structures and could be adapted for design applications or parametric studies. In particular, it can be used to calculate mechanical quantities like acceleration levels in the ballast layer, which could be used as a criterion to evaluate the stability of the ballast (i.e. the risk of settlements) or the maximum tensile strains in the asphalt layer (if applicable), which can be used to evaluate its fatigue life.

DISCLOSURE STATEMENT

The authors reported no potential conflict of interest.

FUNDING

The authors would like to acknowledge the different partners of the project “Instrumentation of HSL BPL”: Railenium, Eiffage, SNCF Réseau and Setec.

REFERENCES

CEREMA-IDRRIM. Diagnostic et conception des renforcements de chaussées. 2016

Chabot A., Chupin O., Deloffre L., & Duhamel D. Viscoroute 2.0 A : Tool for the simulation of moving load effects on asphalt pavement. Road Materials and Pavement Design 2010. 11(2), 227–250.

Chailleux E., Such C., Ramond G., de La Roche C. A mathematical-based master-curve construction method applied to complex modulus of bituminous materials. International Journal Road Materials and Pavement Design 2006. Vol 7, Special Issue EATA, pp 75-92

Chupin O., Martin A., Piau J.-M., & Hicher P.-Y. Calculation of the dynamic response of a viscoelastic railway structure based on a quasi-stationary approach. International Journal of Solids and Structures 2014. *51*(13), 2297-2307.

Chupin O., Chabot A., Piau J.-M., & Duhamel D. Influence of sliding interfaces on the response of a layered viscoelastic medium under a moving load. International Journal of Solids and Structures 2010. 47(25-26), 3435–3446. https://doi.org/10.1016/j.ijsolstr.2010.08.020

Chupin O., & Piau J.-M. Modeling of the dynamic response of ballast in high-speed train structures. 8th International Conference on Structural Dynamics. 2011a. pp-712.

Chupin O., & Piau J.-M. Modélisation de la réponse dynamique d’une structure ferroviaire multicouche sous chargement roulant. Congrès Français de Mécanique (CFM 2011). 2011b, 6p.

Chupin O., Martin A., Piau J.-M., Hicher P.-Y., Calculation of the dynamic response of a viscoelastic railway structure based on a quasi-stationary approach, International Journal of Solids and Structures (2014) 51, 2297–2307

Chupin O., Piau J.M., Martin A., Dano C., Hicher P.Y. Investigation of the reversible response of track ballast considering complementary approaches. Transportation Geotechnics. 2021, 26, 100436. https://doi.org/10.1016/j.trgeo.2020.100436

Connolly D. P., Kouroussis G., Giannopoulos A., Verlinden O., Woodward P. K., & Forde M. C. Assessment of railway vibrations using an efficient scoping model. Soil Dynamics and Earthquake Engineering. 2014 *58*, 37–47.

Duhamel D., Chabot A., Tamagny P., & Harfouche L. ViscoRoute : Visco-elastic modeling for asphalt pavements. Bulletin des Laboratoires des Ponts et chaussées. 2005, *258*, 89–103.

Filippov A. P. Steady state vibrations of an infinite beam on an elastic half-space subjected to a moving load. Izvestija AN SSSR OTN Mehanika i Mashinostroenie. 1961 6, 97–105.

Fortunato E. M. C. Renovação de plataformas ferroviárias : Estudos relativos à capacidade de carga. FEUP - Faculdade de Engenharia da Universidade do Porto. 2005

Hall L. Simulations and analyses of train-induced ground vibrations in finite element models. Soil Dynamics and Earthquake Engineering. 2003, 23(5), 403–413.

Heckl M. A. COUPLED WAVES ON A PERIODICALLY SUPPORTED TIMOSHENKO BEAM. Journal of Sound and Vibration. 2002, 252(5), 849-882. https://doi.org/10.1006/jsvi.2001.3823

Huet C. Étude par une méthode d'impédance du comportement viscoélastique des matériaux hydrocarbonés [Study of the viscoelastic behavior of bituminous mixes by method of impedance]. 1963 [PhD Thesis] (in French).

Huet C. Coupled size and boundary-condition effects in viscoelastic heterogeneous and composite bodies. Mechanics of Materials. 1999, 31(12), 787–829.

Karrech A. Comportement des matériaux granulaires sous vibration-Application au cas du ballast. 2007, [PhD Thesis] (in French).

Khairallah D. Analyse et modélisation de comportement mécanique de structures de voies ferrées avec sous-couche bitumineuse. 2019, [PhD Thesis] (in French).

Khairallah D., Blanc J., Cottineau L. M., Hornych P., Piau J.-M., Pouget S., Hosseingholian M., Ducreau A., & Savin F. Monitoring of railway structures of the high speed line BPL with bituminous and granular sublayers. Construction and Building Materials. 2019a, 211, 337-348. https://doi.org/10.1016/j.conbuildmat.2019.03.084

Khairallah D., Blanc J., Hornych P., Piau J.-M., Cottineau L.-M., Pouget S., Ducreau A., Savin F., & Hosseingholian M. Influence of the Bituminous Layer on Temperature and Water Infiltration in Railway Structures of the Bretagne–Pays de la Loire High-Speed Line. Journal of Testing and Evaluation. 2019b, 48(1), 134-149. https://doi.org/10.1520/JTE20180894

Khairallah D., Chupin O., Blanc J., Hornych P., Piau J.M., Ramirez D., Ducreau A., Savin F. Monitoring and Modeling of Railway Structures of the High Speed Line BPL with Asphalt Concrete Underlayment, Transportation Research Record. 2020, 2674(12), 600–607, DOI: 10.1177/0361198120960472

Kouroussis G., Verlinden O., & Conti C. Free field vibrations caused by high-speed lines : Measurement and time domain simulation. Soil Dynamics and Earthquake Engineering. 2011, 31(4), 692–707.

Krylov V. V. Generation of ground vibrations by superfast trains. Applied Acoustics. 1995, 44(2), 149-164. https://doi.org/10.1016/0003-682X(95)91370-I

Lambert L., Le Dizes A., Giraud H., Robinet A., & Talfumière V. 40 lat doświadczenia w budowie linii dużych prędkości. Planowanie tras, podłoże i hydrotechnika : Praktyka, wytyczne i rozwój. Zeszyty Naukowo-Techniczne Stowarzyszenia Inżynierów i Techników Komunikacji w Krakowie. Seria: Materiały Konferencyjne. 2011

Le Cam V, Lemarchand L., Martin W., & Bonnec N. Improving wireless sensor behavior by means of generic strategies. Structural Health Monitoring. 2010, 1, 696-703.

Le Cam V., Cottineau L., Lemarchand L., & Bourquin F. Design of a generic smart and wireless sensors network–Benefits of emerging technologies. Structural Health Monitoring. 2008, 1(1), 598-605.

Liu X., Zhao P., & Dai F. Advances in design theories of high-speed railway ballastless tracks. Journal of Modern Transportation. 2011, 19(3), 154–162.

Martin A. Analy*se numériq*ue de la réponse dynamique de structures ferroviaires. Application à la réduction des désordres géométriques induits dans les couches de ballast des Lignes à Grande Vitesse. 2014, [PhD Thesis] (in French).

Nielsen J. C., & Igeland A. Vertical dynamic interaction between train and track influence of wheel and track imperfections. Journal of sound and vibration. 1995, 187(5), 825–839.

O'Brien J., & Rizos D. A 3D BEM-FEM methodology for simulation of high speed train induced vibrations. Soil Dynamics and Earthquake Engineering. 2005, 25, 289-301. https://doi.org/10.1016/j.soildyn.2005.02.005

Paixão A., Fortunato E., & Calçada R. The effect of differential settlements on the dynamic response of the train–track system : A numerical study. Engineering Structures. 2015, 88, 216–224.

Preteseille M., & Lenoir T. Mechanical fatigue behavior in treated/stabilized soils subjected to a uniaxial flexural test. International Journal of Fatigue. 2015, 77, 41–49.

Preteseille M., Lenoir T., Gennesseaux E., & Hornych P. Structural test at the laboratory scale for the utilization of stabilized fine-grained soils in the subgrades of High Speed Rail infrastructures : Analytical and numerical aspects. Construction and Building Materials. 2014, 61, 164–171.

Rose J. G., & Souleyrette R. R. Asphalt Railway Trackbeds : Recent Designs, Applications and Performances. Proceedings of the American Railway Engineering and Maintenance-of-Way Association. 2015, Conference, Minneapolis, MN.

Saussine G., & Néel O. High speed regulation in extreme conditions. Proceedings of the Second International Conference on Railway Technology: Research, Development and Maintenance. 2014

Sayegh G. Variation des modules de quelques bitumes purs et bétons bitumineux. 1965, [PhD Thesis]. Thèse de doctorat d'ingénieur, Faculté des Sciences de l'Université de Paris.

Semblat J. F., & Pecker A. Waves and Vibrations in soils : Earthquakes. Traffic, Shocks, Construction works. 2009

Sheng X., Li M., Jones C. J. C., & Thompson D. Using the Fourier-series approach to study interactions between moving wheels and a periodically supported rail. Journal of Sound and Vibration. 2007, 303, 873-894. https://doi.org/10.1016/j.jsv.2007.02.007

Voivret C., Nhu V. H., & Perales R. Discrete element method simulation as a key tool towards performance design of ballasted tracks. International Journal of Railway Technology. 2016, 5, 83–98.

Voivret C., Perales R., & Saussine G. Ballasted track maintenance with a multi-unit tamping machine: A numerical discrete efficiency comparison. Proceedings of the Second International Conference on Railway Technology: Research, Development and Maintenance. 2014, 53.

Vostroukhov A. V., & Metrikine A. Periodically supported beam on a visco-elastic layer as a model for dynamic analysis of a high-speed railway track. International Journal of Solids and Structures. 2003, 40, 5723-5752. https://doi.org/10.1016/S0020-7683(03)00311-1

Xu Q., Xiao Z., Liu T., Lou P., & Song X. Comparison of 2D and 3D prediction models for environmental vibration induced by underground railway with two types of tracks. Computers and Geotechnics. 2015, 68, 169–183.

Yang X., Gu S., Zhou S., Yang J., Zhou Y., & Lian S. Effect of track irregularity on the dynamic response of a slab track under a high-speed train based on the composite track element method. Applied Acoustics. 2015, 99, 72-84. https://doi.org/10.1016/j.apacoust.2015.05.009

Zhou T., Hu B., Sun J., & Liu Z. Discrete element method simulation of railway ballast compactness during tamping process. The Open Electrical & Electronic Engineering Journal. 2013, 7, 103–109.